Regional Dendritic and Spine Variation in Human Cerebral Cortex: a Quantitative Golgi Study

Bob Jacobs, Matthew Schall[1], Melissa Prather[2], Elisa Kapler, Lori Driscoll[3], Serapio Baca[4], Jesse Jacobs, Kevin Ford, Marcy Wainwright[5] and Melinda Treml

Laboratory of Quantitative Neuromorphology, Department of Psychology, The Colorado College, 14 E. Cache La Poudre, Colorado Springs, CO 80903, [1]UniFocus, 1330 Capital Parkway, Carrolton, TX 75006, [2]Department of Neuroscience, University of California, Davis, CA 95616, [3]Department of Psychology, Cornell University, Ithaca, NY 14853, [4]Neurosciences Graduate Program, University of California, San Diego, CA 92093-0357 and [5]Department of Neurobiology and Anatomy, University of Texas, Houston, TX 77030, USA

The present study explored differences in dendritic/spine extent across several human cortical regions. Specifically, the basilar dendrites/spines of supragranular pyramidal cells were examined in eight Brodmann's areas (BA) arranged according to Benson's (1993, Behav Neurol 6:75–81) functional hierarchy: primary cortex (somatosensory, BA3-1-2; motor, BA4), unimodal cortex (Wernicke's area, BA22; Broca's area, BA44), heteromodal cortex (supplementary motor area, BA6β; angular gyrus, BA39) and supramodal cortex (superior frontopolar zone, BA10; inferior frontopolar zone, BA11). To capture more general aspects of regional variability, primary and unimodal areas were designated as low integrative regions; heteromodal and supramodal areas were designated as high integrative regions. Tissue was obtained from the left hemisphere of 10 neurologically normal individuals (M_{age} = 30 ± 17 years; five males, five females) and stained with a modified rapid Golgi technique. Ten neurons were sampled from each cortical region (n = 800) and evaluated according to total dendritic length, mean segment length, dendritic segment count, dendritic spine number and dendritic spine density. Despite considerable inter-individual variation, there were significant differences across the eight Brodmann's areas and between the high and low integrative regions for all dendritic and spine measures. Dendritic systems in primary and unimodal regions were consistently less complex than in heteromodal and supramodal areas. The range within these rankings was substantial, with total dendritic length in BA10 being 31% greater than that in BA3-1-2, and dendritic spine number being 69% greater. These findings demonstrate that cortical regions involved in the early stages of processing (e.g. primary sensory areas) generally exhibit less complex dendritic/spine systems than those regions involved in the later stages of information processing (e.g. prefrontal cortex). This dendritic progression appears to reflect significant differences in the nature of cortical processing, with spine-dense neurons at hierarchically higher association levels integrating a broader range of synaptic input than those at lower cortical levels.

Introduction

The cerebral cortex has historically been parceled according to cyto- and myelo-architectonic criteria (Brodmann, 1909; Vogt, 1910), with little attention to potential regional variation in dendritic systems. Although the qualitative characteristics of cortical pyramidal neurons have been relatively well documented (Ramón y Cajal, 1909, 1911; Ramón-Moliner, 1962), much less is known about their quantitative variation across cortical areas because most studies have focused on only one region at a time. Nevertheless, in the last decade, since Scheibel *et al.* (Scheibel *et al.*, 1985, 1990) suggested a positive relationship between dendritic extent and functional complexity in human cortex, several quantitative neuromorphological investigations have begun to document regional dendritic variation. The present study extends this concept of regional cortical variability by exploring the degree to which the basilar dendritic and spine systems of supragranular pyramidal neurons vary across eight regions of the human cerebral cortex.

Both human and non-human animal research indicate that regional dendritic variation may be extensive, with profound functional implications for cortical processing. In humans, Jacobs *et al.* (Jacobs *et al.*, 1997) noted that the basilar dendrites and associated spines in Brodmann's area (BA) 10 were significantly more extensive than those in BA18. Functionally, the more limited dendritic systems in BA18 neurons appear to correspond with more discrete sampling of afferent information (i.e. smaller receptive fields). In contrast, the more complex dendritic arrays in BA10 neurons may facilitate a broader sampling of afferent information, thereby potentially increasing their integrative capacity. In an extensive series of studies on hierarchically arranged visual pathways in monkeys, Elston and Rosa (Elston *et al.*, 1996; Elston and Rosa, 1997, 1998a,b) have documented a caudal–rostral progression in dendritic field size and spine number, suggesting a more extensive input sampling by dendritic systems at higher levels. These data correspond with demonstrated size increases in intrinsic axonal clusters across the visual cortical hierarchy (Amir *et al.*, 1993).

The present investigation provides a broader view of regional variability in humans than past research by incorporating a more extensive sampling of cortical areas. To this end, the current study explores the morphological underpinnings of the functional cortical hierarchy proposed by Benson (Benson, 1993, 1994). Benson's hierarchy draws heavily on the sensory-fugal gradients of cortical connectivity proposed by Mesulam (Mesulam, 1985), which have recently undergone considerable elaboration (Mesulam, 1998). In Benson's useful hierarchical schema, the cerebral cortex is classified into four divisions based on clinical/anatomical correlations. Each of these cortical types represents a progressively more complex level of neural processing: *primary* cortex is involved in the initial processing of sensory impulses, or the final output stage for motor functions; *unimodal* regions discriminate, categorize and integrate information within a single modality to form a percept of the same modality; *heteromodal* cortex compares a particular percept with previously experienced percepts from other modalities to form complex multimodal percepts; and *supramodal* association regions are involved in executive control of cognitive networks.

Although these divisions and their anatomical boundaries are far from absolute, especially given the interconnectional complexity of cortical circuitry, these categories do provide an initial framework for examining dendritic/spine systems *vis-à-vis* a functional hierarchy. In the current study, two

© Oxford University Press 2001. All rights reserved.

Table 1
Subject summary

Subject[a]	Body weight (in kg)	Autolysis time (in h)	Cause of death	Occupation (education)[b]
F11	–	13	malignant lymphoma	middle school student (MS)
M14	47	14	cardiac arrhythmia	high school student (HS)
F15	–	8	acute myelogenous leukemia	high school student (HS)
F22	–	1	mucopolysacchridosis type VI	–
M23	82	12	motor vehicle accident	–
F32	77	20	coronary artery heart disease	nutritionist (UNI)
M32	74	9	asphyxia (suicide)	–
F34	88	14.5	heroin overdose	Computer programmer (UNI)
M50	87	22	motor vehicle accident	truck driver
M69	58	7	prostate cancer	maintenance worker

[a]Subjects are referred to by gender (M = male; F = female) and by age in years. For example, F11 refers to an 11-year-old female. Note also that some tissue samples (namely, BA10) from all subjects except F11 and F15 were used previously (Jacobs *et al.*, 1997).

[b]Abbreviations: MS = middle school; HS = high school; UNI = university.

Brodmann's areas were chosen to represent each level of Benson's schema: primary cortex (somatosensory, BA3-1-2; motor, BA4), unimodal cortex (Wernicke's area, BA22; Broca's area, BA44), heteromodal cortex (supplementary motor area, BA6β; angular gyrus, BA39) and supramodal cortex (superior frontopolar zone, BA10; inferior frontopolar zone, BA11). In order to capture more general aspects of regional cortical variation, primary and unimodal areas were designated as relatively low integrative regions; heteromodal and supramodal areas were designated as relatively high integrative regions. Based on the above evidence and on preliminary research (Baca *et al.*, 1995; Prather *et al.*, 1997), dendritic measures were expected to increase in a relatively consistent manner from primary to supramodal cortical regions, with dendritic/spine systems in high integration regions being significantly more complex than those in low integration regions.

Materials and Methods

Subjects

Tissue was obtained from 10 neurologically normal subjects (M_{age} = 30 ± 17 years; five males: M_{age} = 38 ± 20 years; five females: M_{age} = 23 ± 9 years; see Table 1). Autolysis time (AT) averaged 12 ± 6 h (range: 1–22 h); all brains were immersion fixed in 10% neutral buffered formalin for an average of 32 ± 16 days prior to staining. Tissue was provided by (i) Dr D. Bowerman, of the El Paso County coroner's office (six brains); and (ii) Drs E. Orsini, W. Tyson and S. Caldwell, of Denver's Children's Hospital (four brains). All possible historical information (e.g. age, gender, cause of death, agonal period) on each subject was obtained from autopsy reports and medical records. Tissue was excluded if there were any signs of trauma, cerebral edema or chronic illness with central nervous system involvement. The research protocol was approved by The Colorado College Human Subjects Review Board (#H94-004).

Tissue Selection and Processing

A tissue block (1–2 cm along the long axis of the gyrus) was removed from the left hemisphere in each of the following regions: BA3-1-2, BA4, BA22, BA44, BA6β, BA39, BA10 and BA11 (see Fig. 1). The relative location and anatomical characteristics of each of these regions is briefly described below:

BA3,1,2 and BA4

BA3-1-2 and BA4 were removed from adjacent regions of the post- and pre-central gyri, respectively (~2–3 cm from the midline along the dorsolateral convexity). This location generally represented the arm/hand region in the classical somotopically organized homunculi maps (Penfield and Boldrey, 1937), and appears consistent with modern three-dimensional characterizations of this region (Sastre-Janer *et al.*, 1998). Sections removed from the post-central gyrus were not further subdivided by cytoarchitectonic criteria, although, given that cells were sampled from the crown of the gyrus, it is likely that most neurons were from BA1 and BA2. The agranular, pre-central gyrus sections often contained diffuse aggregations of Betz cells.

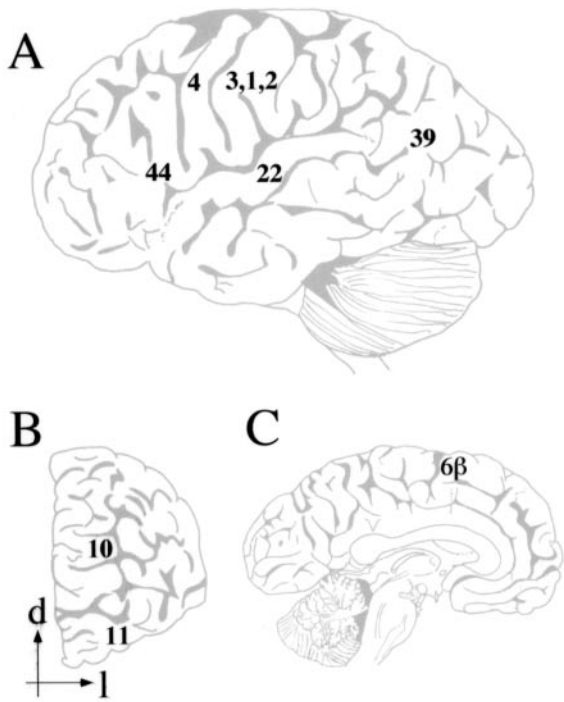

Figure 1. (*A*) Lateral, (*B*) frontal and (*C*) medial views of the left hemisphere illustrating the relative position of tissue blocks (listed by Brodmann's areas, BA) in the present sample. BA3-1-2, BA4, BA22 and BA44 were classified as low integration regions; BA6β, BA10, BA11 and BA39 were classified as high integration regions. Note that these depictions do not capture the considerable morphological variation that typifies individual brains. d = dorsal, l = lateral.

BA22

BA22 constituted classical Wernicke's area (area TA1, von Economo and Koskinas, 1925), and was removed according to established criteria: the anterior edge of the block was adjacent with the posterior edge of the antero-lateral tip of the primary transverse gyrus of Heschl (Jacobs and Scheibel, 1993). Cytoarchitectonically, this area represents typical six-layered isocortex and is characterized by large pyramidal cells in layer IIIc (Braak, 1980).

BA44

Classical Broca's area is composed of both BA44 and BA45, which appear to be heterogeneous in terms of architectonic and functional criteria. The present sample was limited to tissue from the opercular portion of the inferior frontal gyrus, corresponding to the agranular fronto-opercular zone of Sanides (Sanides, 1962). This sampling is consistent with recent quantitative mapping of this region (Amunts *et al.*, 1999).

BA6β

BA6β constituted the supplementary motor region, and was removed from the superior frontal gyrus anterior to the paracentral lobule on the medial surface of the hemisphere. This midline area thus represents the superior portion of Braak's (Braak, 1980) frontal magnopyramidal region.

BA39

BA39 constituted the angular gyrus, and was removed from the lobule surrounding the ascending posterior segment of the parallel sulcus. Cytoarchitectonically, this region is characterized by a narrow granular layer IV and a relative 'clearing' of layers IIIb and V, which provide it with its overall eulaminate quality and distinct horizontal lamination (Eidelberg and Galaburda, 1984).

BA10 and BA11

Both BA10 and BA11 constitute association isocortex with a clear inner granular layer. BA10 was removed superiorly from the frontal pole, ~1.5 cm from the midline and 3–4 cm superior to the orbitomedial surface. BA11 was removed more inferiorly, ~1.5 cm lateral from the midline and along the anterior-most portion of the lateral orbital gyrus. It should be noted that Brodmann's (Brodmann, 1909) exploration of these regions was not as detailed as modern analyses (Cavada *et al.*, 2000; Van Hoesen *et al.*, 2000). In the present study, BA10 and BA11 correspond respectively to the superior and inferior portions of the granular frontopolar zone of Sanides (Sanides, 1962). In more recent terminology, the present sampling of BA11 corresponds to area FP in the map of Hof *et al.* (Hof *et al.*, 1995), and to area 10o in the schema of Öngür and Price (Öngür and Price, 2000). However, for consistency, Brodmann's nomenclature is used throughout the present analysis.

Tissue blocks were coded to prevent experimenter bias, trimmed to 3–5 mm in antero-posterior thickness, and processed by a modified rapid Golgi technique (Scheibel and Scheibel, 1978). To be consistent with previous research (Jacobs *et al.*, 1997), processed tissue was serially sectioned at 120 μm with a vibratome such that the preparation was vertical to the pial surface and perpendicular to the long axis of the gyrus. Adjacent tissue blocks were sectioned at 50 μm and stained with a modified cresyl echt violet technique (Gridley, 1960), which permitted cytoarchitectonic comparisons for routine control purposes and for measures of laminar depth (expressed as the mean of five sample measurements taken across the crown of the gyrus).

Cell Selection Criteria and Dendritic/Spine Quantification

Ten relatively isolated supragranular pyramidal cells per tissue block (i.e. 80 cells per brain) were randomly chosen for analysis following previously established criteria (Jacobs *et al.*, 1997). Briefly, selected neurons appeared fully impregnated, and relatively complete, with the soma located centrally within the 120 μm section depth and the apical dendrite perpendicular to the pial surface. To assure a relatively homogeneous cell population, all cells were sampled no further than 1.5 cm vertically from the tip of the gyral crown, with a running average of soma depth from the pial surface maintained as cells from each cortical area were drawn. Magnopyramidal neurons were not traced, nor was a distinction made between subtypes of pyramidal neurons.

Cells were quantified along *x*-, *y*- and *z*-coordinates on a Neurolucida system (Microbrightfield, Inc.) interfaced with an Olympus BH-2 microscope under a planachromat ×40 (0.70) dry objective. Tracings began with the soma, which was traced at its widest point in the two-dimensional plane to provide an estimate of its cross-sectional area. After drawing the apical shaft, basilar dendrites were traced in their entirety along with all visible spines. No distinction was made between different spine types. Dendritic processes were not followed into adjacent sections nor was dendritic diameter examined. Broken tips and unclear terminations were indicated as incomplete endings. Of the 43 954 dendritic segments quantified, 45% were intermediate segments. With regard to terminal segments, 45% were complete and 55% were incomplete. Sectioned segments were not differentially analyzed because elimination of cells with incomplete segments would have biased the sample towards smaller neurons (Uylings *et al.*, 1986).

Cells were traced by 12 individuals. Intrarater reliability was determined by having each rater trace the same dendritic system (including somata and spines) 10 times over a 2–4 day period. There was little variation in tracings; the average coefficient of variation (CV) across all raters for soma size, total dendritic length and dendritic spine number, was 5, 3 and 6%, respectively. To further test intrarater reliability, a split plot design ($\alpha = 0.05$) compared the first five tracings with the second five tracings; no significant difference was found within raters for any of these measures. To maximize interrater reliability, all raters were normed before quantification by comparing their tracings over a 1–2 week period to those of the primary investigator (B.J.). In tracings of 10 different dendritic systems, Pearson product correlations across soma size, total dendritic length and dendritic spine number averaged 0.93, 0.99 and 0.97, respectively. The tested agreement among raters was further evaluated by using an analysis of variance (ANOVA; $\alpha = 0.05$), which indicated no significant difference among raters on these measures. Finally, all tracings of neurons were re-examined by the primary investigator to assure quality control.

Dependent Dendritic/Spine Measures

Dendritic systems were quantified according to a centrifugal nomenclature (Bok, 1959; Uylings *et al.*, 1986): dendritic branches arising from the soma are first-order segments until they bifurcate into second-order segments, which branch into third-order segments, and so on. Five measures (represented as mean ± SEM) characterized each cell's dendritic system. Total dendritic length (TDL) refers to the summed length of dendritic segments. Mean segment length (MSL) represents the mean length of dendritic segments. Dendritic segment count (DSC) refers to the number of dendritic segments. Dendritic spine number (DSN) refers to the sum of all spines on dendritic segments. Dendritic spine density (DSD) represents the average number of spines per micron of dendritic length. It should be noted here that many of these measures are interrelated (e.g. TDL is the product of MSL and DSC values).

Independent Variables and Statistical Analyses

Individual Brodmann's areas provided one independent measure for the present study. In addition, to capture more general aspects of regional variation, Brodmann's areas were grouped in the following manner: areas representing primary and unimodal cortices (BA3-1-2, 4, 22 and 44) were designated as low integrative regions; areas representing heteromodal and supramodal cortices (BA6β, 10, 11 and 39) were designated as high integrative regions.

The raw dendritic data set was aggregated by neuron (Cell). Separate analyses subsequently evaluated the effects of (i) Brodmann's areas (Brodmann) and (ii) integration level (Integration) on each of the five dependent measures by using a nested ANOVA design (Proc Nested; SAS, 6.08 for UNIX). In this model, Cell was nested within Brodmann or Integration, each of which was nested within Brain. Briefly, this is ostensibly a nested, repeated measures design, whereby each dependent measure is afforded its own nested analysis, thereby increasing the ability to identify how much each independent variable contributes to the values found for the dependent measures. Because this design analyzed one dependent variable at a time, a Bonferroni–Dunn correction ($\alpha = 0.01$) was used to maintain an experimentwise alpha of 0.05.

Results

Summary of Neuronal Sample

Golgi-impregnated tissue did not exhibit the autolytic changes (e.g. irregular varicose enlargements, constriction of dendrites) described by Williams *et al.* (Williams *et al.*, 1978). Moreover, there were no significant correlations between autolysis time and any of the dependent measures [TDL: $r(800) = -0.003$;

MSL: $r(800) = 0.053$; DSC: $r(800) = 0.039$; DSN: $r(800) = -0.108$; DSD: $r(800) = -0.106$]. Several measures taken during data collection served as guidelines to minimize variability in the neuronal sampling procedure: (i) soma depth from pial surface; (ii) soma size; and (iii) laminar thickness. To explore further the relationship among these measures, two-tailed Pearson product–moment correlations based on the 800 sampled neurons were calculated [because of multiple correlations, a Bonferroni–Dunn correction ($\alpha = 0.001$) was used to maintain an experimentwise alpha of 0.05].

Soma Depth

The average soma depth for sampled neurons varied only slightly among Brodmann's areas (from 800.1 μm in BA10 to 852.7 μm in BA44), and was thus very similar between the two integration levels (Table 2). This sampling placed the majority of somata in upper layer III. Soma size increased slightly, but significantly with soma depth [$r(800) = 0.26$, $P < 0.0001$]. There was also a slight positive relationship between soma depth and TDL [$r(800) = 0.15$, $P < 0.0001$], underscoring the necessity of controlling soma depth.

Soma Size

Most sampled neurons were small- to medium-sized pyramidal cells, with the mean soma size being slightly larger in high than in low integration regions (Table 2). As soma size increased, so did TDL [$r(800) = 0.31$, $P < 0.0001$], and DSC [$r(800) = 0.32$, $P < 0.0001$], indicating that larger somata generally exhibited more complex dendritic arbors.

Laminar Thickness

Overall laminar and cortical thickness appeared roughly comparable between the two integration levels (Table 2). The cortex was thickest in BA4 (3.8 mm) and thinnest in BA10 (3.1 mm). The present laminar values are generally consistent with those of previous cytoarchitectonic findings for these regions (Brodmann, 1909; von Economo and Koskinas, 1925).

Dendrite and Spine Systems

Photomicrographs of selected Golgi preparations indicate the overall quality of the stain (Fig. 2). In general, despite considerable interindividual variability, the present results indicate significant differences among Brodmann's areas in the predicted direction, with high integration regions being significantly more complex than low integration regions. Within this classification, overall TDL variability within the four high integration regions (CV = 27%) was slightly less pronounced than TDL variability within the four low integration regions (CV = 32%), which was expected given that the low integration grouping contained not only homotypical but also heterotypical isocortical areas. These regional hierarchical differences are depicted in sample Neurolucida tracings from two individuals: an 11-year-old female (Fig. 3) and a 50-year-old male (Fig. 4). A more detailed analysis of each dependent measure is provided below.

Dendritic Length

There was a significant difference for both TDL [$F(70,720) = 3.66$, $P < 0.0001$] and MSL [$F(70,720) = 3.17$, $P < 0.0001$] across Brodmann levels. A considerable spread in TDL obtained among Brodmann's areas (Fig. 5*A*), with the most complex region (BA10; 4,193 μm/cell) being 31.4% higher than the least complex region (BA3-1-2; 3,191 μm/cell). Differences between Brodmann's areas were somewhat attenuated for MSL (Fig. 6*A*), with the most complex region (BA6β; 73 μm/cell) being only 14.4% greater than the least complex region (BA3-1-2; 64 μm/cell). In terms of the initial classification of these regions, the following ranking obtained for both TDL and MSL: primary < unimodal < supramodal < heteromodal. The values for heteromodal and supramodal regions were nearly identical.

The High Integration level was significantly more complex than the Low Integration level for both TDL [$F(10,180) = 8.95$, $P < 0.0001$] and MSL [$F(10,180) = 5.97$, $P < 0.0001$]. For TDL, the high integration regions were 17.2% higher than the low integration regions (Fig. 5*A*). For MSL, the difference was smaller at 5.6% (Fig. 6*A*). Moreover, MSL was the only measure where a low integration region (namely, BA44) was more complex than a high integration region (namely, BA11). Dendritic envelopes for TDL (Fig. 5*B*) and MSL (Fig. 6*B*) indicated that high integration regions were consistently more complex across almost all dendritic orders, with the greatest difference appearing in third- and fourth-order segments for TDL.

Table 2

Laminar and sampled soma depths (μm) and soma size (μm^2)[a]

	Low integration regions	High integration regions
Layer I/II junction	306 ± 70	314 ± 56
Layer II/III junction	569 ± 102	562 ± 95
Sampled soma depth	838 ± 173	816 ± 181
Sampled soma size	266 ± 95	290 ± 89
Layer III/IV junction	1499 ± 254	1471 ± 170
Gray/white matter junction	3517 ± 527	3304 ± 504

[a]Values represent mean ± SD.

Dendritic Number

There was a significant difference across Brodmann levels for DSC [$F(70,720) = 2.272$, $P < 0.0001$]. As illustrated in Figure 7*A*, the most complex region (BA10; 59 segments/cell) was 19.9% higher than the least complex region (BA3-1-2; 49 segments/cell). The relative complexity of primary, unimodal, heteromodal and supramodal regions was in the predicted direction. The High Integration level was significantly more complex (by 11.1%) in terms of DSC than the Low Integration level [$F(10,180) = 5.58$, $P < 0.0001$]. As with dendritic length, the highest values were exhibited by the middle of the dendritic envelope (especially segment orders 3 and 4), where clear differences emerged between the integration levels (Fig. 7*B*).

Dendritic Spines

The most marked regional cortical differences emerged in dendritic spine measures. There was a significant difference across Brodmann levels for both DSN [$F(70,720) = 7.39$, $P < 0.0001$] and DSD [$F(70,720) = 8.31$, $P < 0.0001$]. A substantial spread in DSN was evident among Brodmann's areas (Fig. 8*A*), with the most complex region (BA10; 1,378 spines/cell) being 68.9% higher than the least complex region (BA3-1-2; 816 spines/cell). Although differences were smaller for DSD (Fig. 9*A*), BA10 (0.26 spines/μm) was still 36.8% higher than BA3-1-2 (0.19 spines/μm). The relative complexity of primary, unimodal, heteromodal and supramodal regions was in the predicted direction for both DSN and DSD.

The High Integration level was significantly more complex than the Low Integration level for both DSN [$F(10,180) = 19.79$, $P < 0.0001$] and DSD [$F(10,180) = 17.68$, $P < 0.0001$]. For DSN, the high integration regions were 32.2% greater than the low integration regions (Fig. 8*A*). For DSD, the difference was smaller

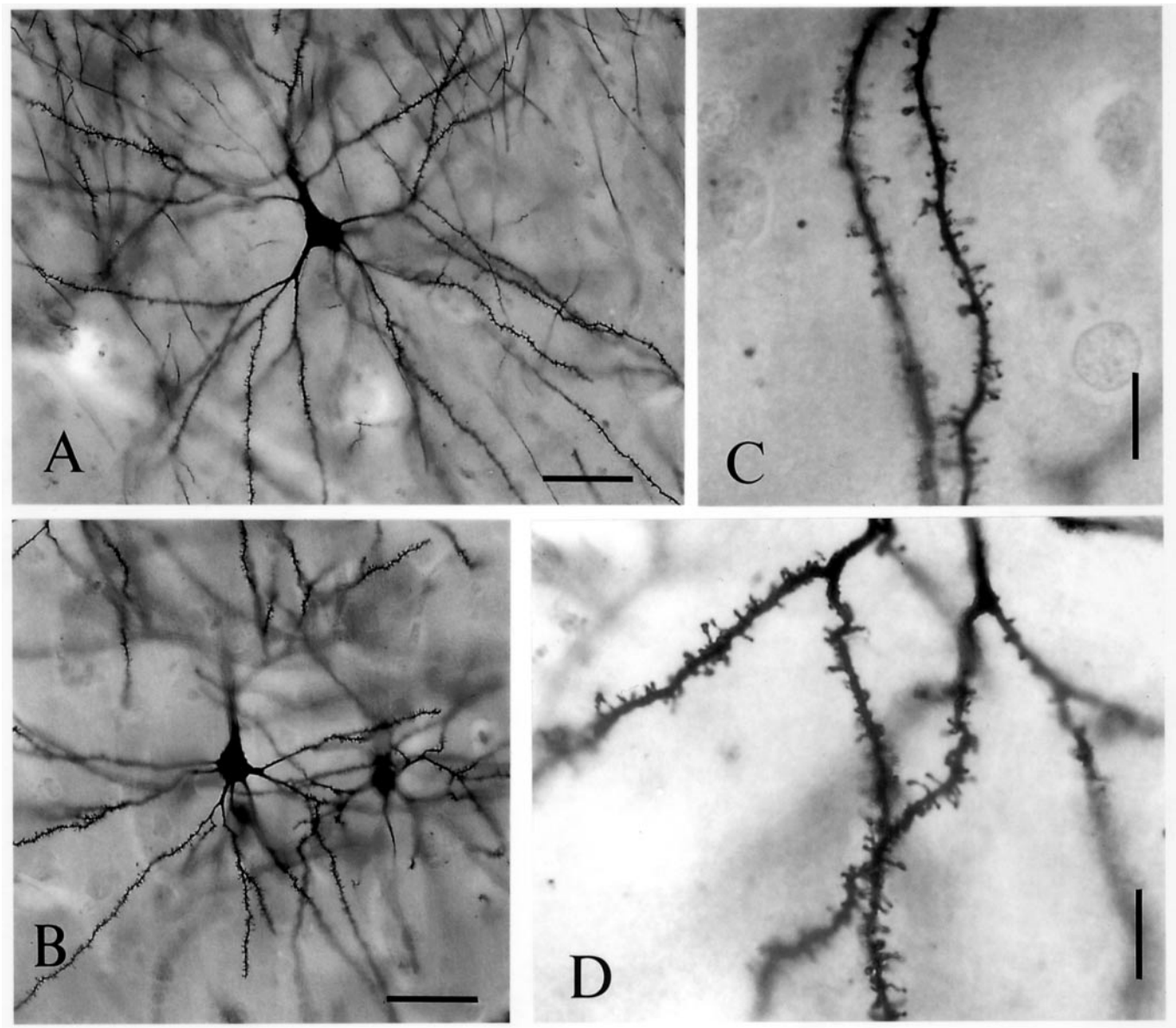

Figure 2. Photomicrographs of supragranular pyramidal cells illustrating the sharp contour and intact quality of the Golgi impregnated dendritic systems. Several cases and Brodmann's areas are represented: (*A*) M32 (= 32-year-old male), BA39; (*B*) F11, BA11; (*C*) F15, BA44; and (*D*) F11, BA3-1-2. For *A* and *B*, scale bars = 50 μm; for *C* and *D*, scale bars = 10 μm.

at 15% (Fig. 9*A*). Much the same as TDL (Fig. 5*B*), DSN values were highest in the middle of the dendritic envelope, which also most clearly differentiated the high and low integration regions (Fig. 8*B*). In contrast, DSD values closely follow the same pattern as MDL measures (Fig. 6*B*), namely increasing somatofugally until the fifth-order segment, and remaining at relatively high levels thereafter (Fig. 9*B*).

Age-related Changes

Because of the age range of the present subjects (58 years), correlations between age and the dependent measures were determined. All correlations except TDL were significant [TDL: $r(800) = 0.014$; MSL: $r(800) = -0.183$, $P < 0.001$; DSC: $r(800) = 0.138$, $P < 0.001$; DSN: $r(800) = -0.440$, $P < 0.001$; DSD: $r(800) = -0.586$, $P < 0.001$], indicating marked decreases in spine measures.

Discussion

The present investigation revealed significant, progressive increases in dendritic/spine extent among hierarchically arranged cortical regions of the human brain. Although the exact sequence of individual Brodmann's areas depended somewhat on the particular aspect of the dendritic tree examined (as illustrated in Figs 5*A*–9*A*), clear patterns did emerge. Consistent with the observation that (i) sensory information undergoes extensive elaboration and modulation during the integration process (Mesulam, 1998), and (ii) the processing demands placed on dendritic systems in various cortical regions substantially influence their ultimate expression (Ramón y Cajal, 1894; Diamond *et al.*, 1964), dendritic/spine systems in the present analysis were generally less complex in low integration regions (primary and unimodal cortices) than in high integration regions (heteromodal and supramodal cortices). Before

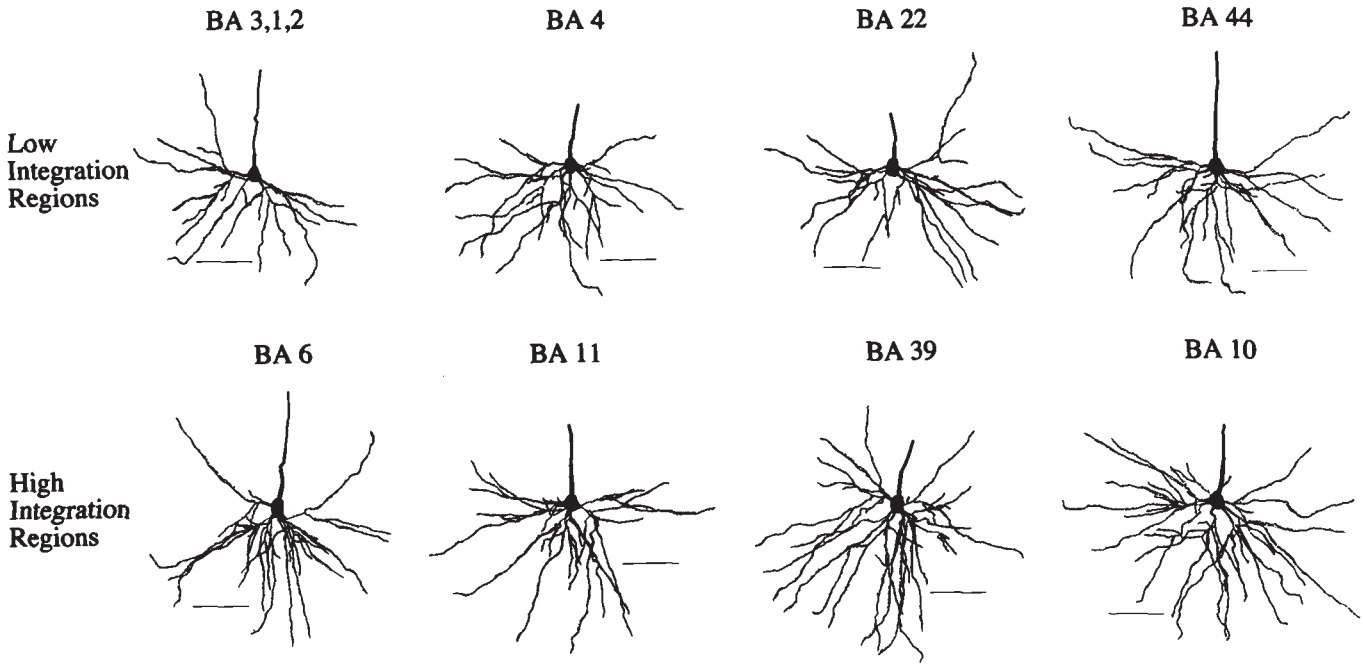

Figure 3. Sample tracings of supragranular pyramidal cells from each Brodmann area (BA) for F11. These regions have been arranged to represent the relative order of dendritic/spine complexity for this individual, with cells in BA3-1-2 being the least complex and cells in BA10 being the most complex. Overall, cells in the low integration regions (BA3-1-2, BA4, BA22 and BA44) exhibited less dendritic branching than cells in the high integration regions (BA6, BA11, BA39 and BA10). Scale bars = 100 μm.

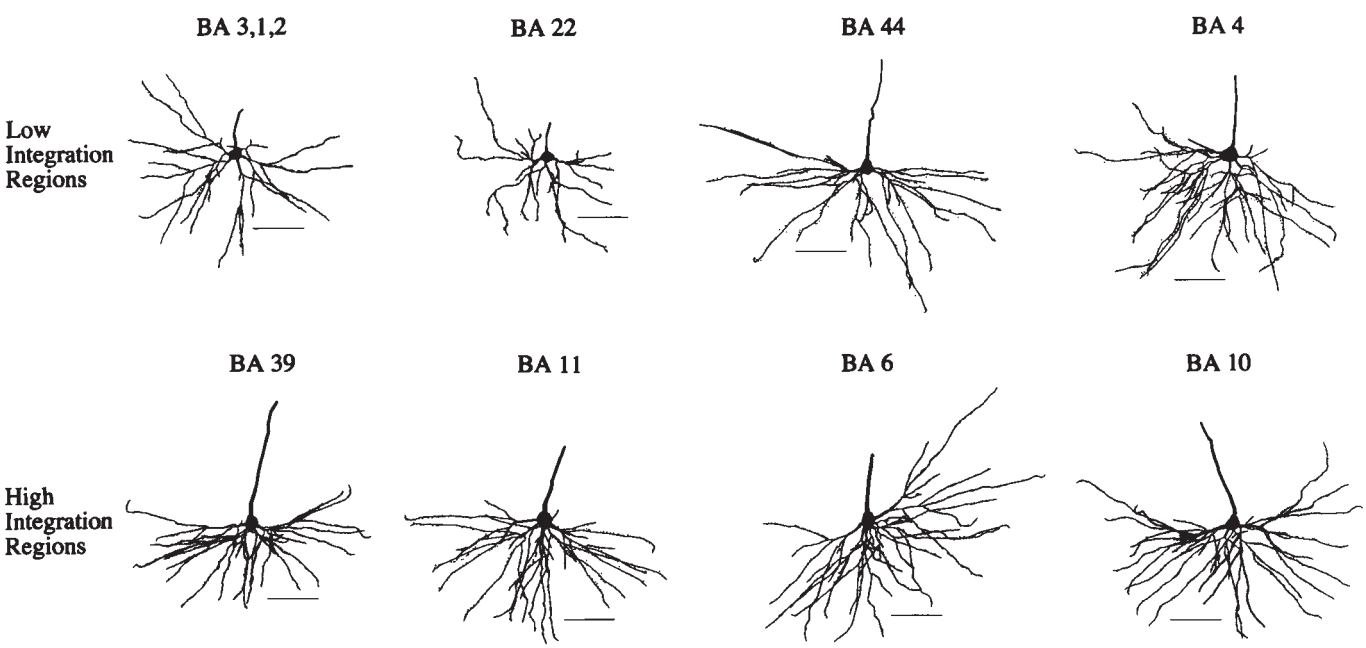

Figure 4. Sample tracings of supragranular pyramidal cells from each Brodmann area (BA) for M50. These regions have been arranged to represent the relative order of dendritic/spine complexity for this individual. As with F11 (Fig. 3), cells in BA3-1-2 were the least complex and cells in BA10 were the most complex. However, note that the relative order of regions within low (BA3-1-2, BA22, BA44, and BA4) and high integration regions (BA39, BA11, BA6, and BA10) differs from F11, illustrating the interindividual differences that characterize human tissue. Scale bars = 100 μm.

discussing these results in detail, several methodological issues need to be addressed.

Methodological Considerations

The implications of the present results are tempered by well-known methodological limitations (e.g. the practical constraints of human research, Golgi stains, small sample sizes and post-mortem delay effects), most of which have been addressed elsewhere (Williams *et al.*, 1978; de Ruiter 1983; Flood, 1993; Jacobs and Scheibel, 1993; Jacobs *et al.*, 1993b, 1997). A primary limitation of the present study is that it did not address potential hemispheric differences, all of which

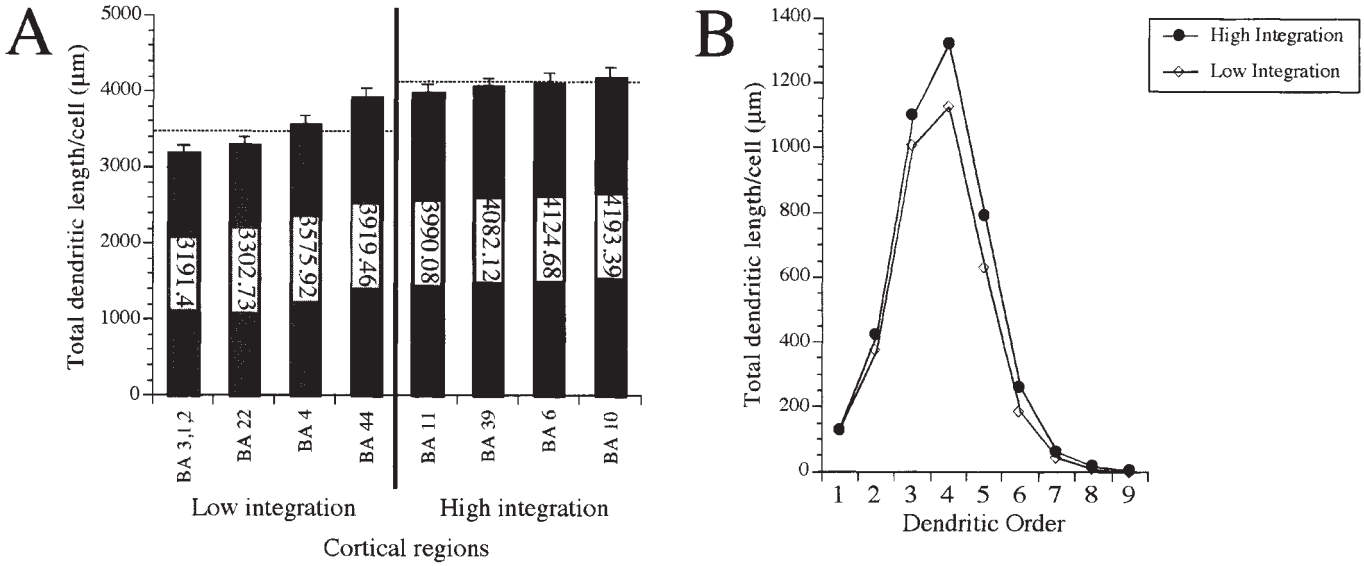

Figure 5. (*A*) Bar graph of the relative total dendritic length (TDL, µm) for each Brodmann area (BA), arranged from lowest (BA3-1-2) to highest (BA10). Areas have been characterized as low (BA3-1-2, BA22, BA4 and BA44) and high integration regions (BA11, BA39, BA6 and BA10), with the average TDL value for each grouping indicated by the dotted lines. Note the relatively higher TDL values for the high integration regions over the low integration regions. Error bars represent SEM. (*B*) Dendritic envelopes for low and high integration regions indicating the greatest differences in third-, fourth- and fifth-order dendritic branches.

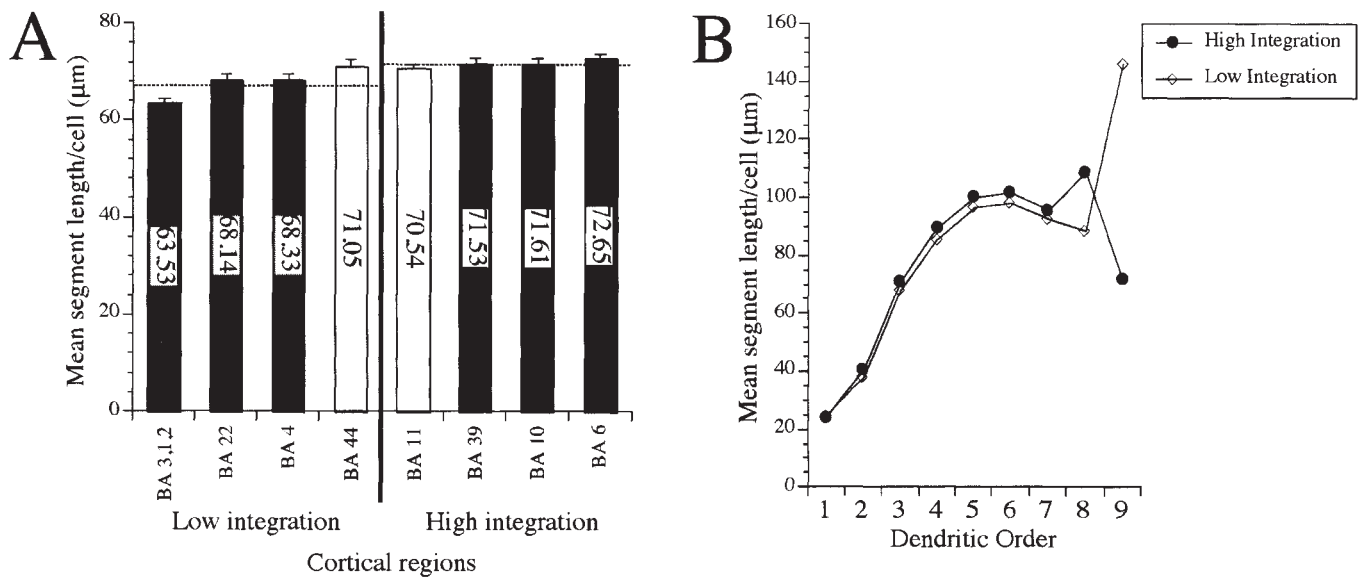

Figure 6. (*A*) Bar graph of the relative mean segment length (MSL, µm) for each Brodmann area (BA), arranged from lowest (BA3-1-2) to highest (BA6). Areas have been characterized as low (BA3-1-2, BA22, BA4 and BA44) and high integration regions (BA11, BA39, BA10 and BA6). MSL is slightly higher for the high integration regions over the low integration regions. Note, however, that BA44 MSL values are higher than BA11 MSL values (white columns). Error bars represent SEM. (*B*) Dendritic envelopes indicating the relative increase in MSL values with each successive dendritic order — until the sixth — for both low and high integration regions.

clearly affect certain aspects of cortical function/organization (Anderson and Rutledge, 1996). Three additional issues require elaboration: (i) dendritic and spine quantification; (ii) individual morphological/cytoarchitectonic variability; and (iii) hierarchical classification of cortical tissue.

Dendritic and Spine Quantification

The present quantification technique provided only a limited view of cortical neuropil. As noted by Jacobs *et al.* (Jacobs *et al.*, 1997), 120 µm sections result in sectioned dendrites. As such, the present dendritic values represent underestimations of actual dendritic extent, particularly with regard to the more distal segments (i.e. sixth-order and higher). Importantly for the present study, the number of incomplete segments (mostly due to sectioning) in high integration regions was 6.6% higher than in low integration regions. Similarly, insofar as spines cannot be visualized directly above or below dendrites with light microscopy, the present spine measures also represent underestimates, especially for thicker dendrites (Horner and Arbuthnott, 1991). Although correction equations (Feldman and Peters, 1979) and three-dimensional reconstructions of dendrites (Belichenko and Dahlström, 1995) may compensate

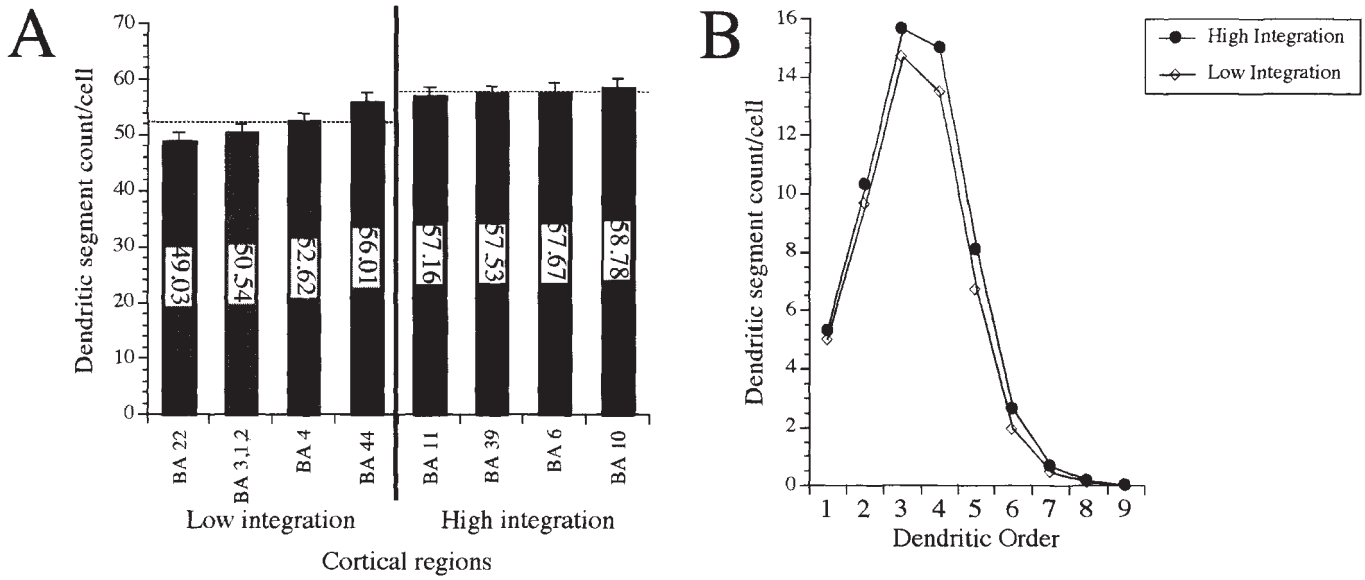

Figure 7. (A) Bar graph of the relative dendritic segment count (DSC) for each Brodmann area (BA), arranged from lowest (BA22) to highest (BA10). Areas have been characterized as low (BA11, BA3-1-2, BA4 and BA44) and high integration regions (BA11, BA39, BA6 and BA10), with the average DSC value for each grouping indicated by the dotted lines. Note the relatively higher DSC values for the high integration regions over the low integration regions. Error bars represent SEM. (*B*) Dendritic envelopes for Low and High Integration regions indicating the greatest differences in third- and fourth-order dendritic branches.

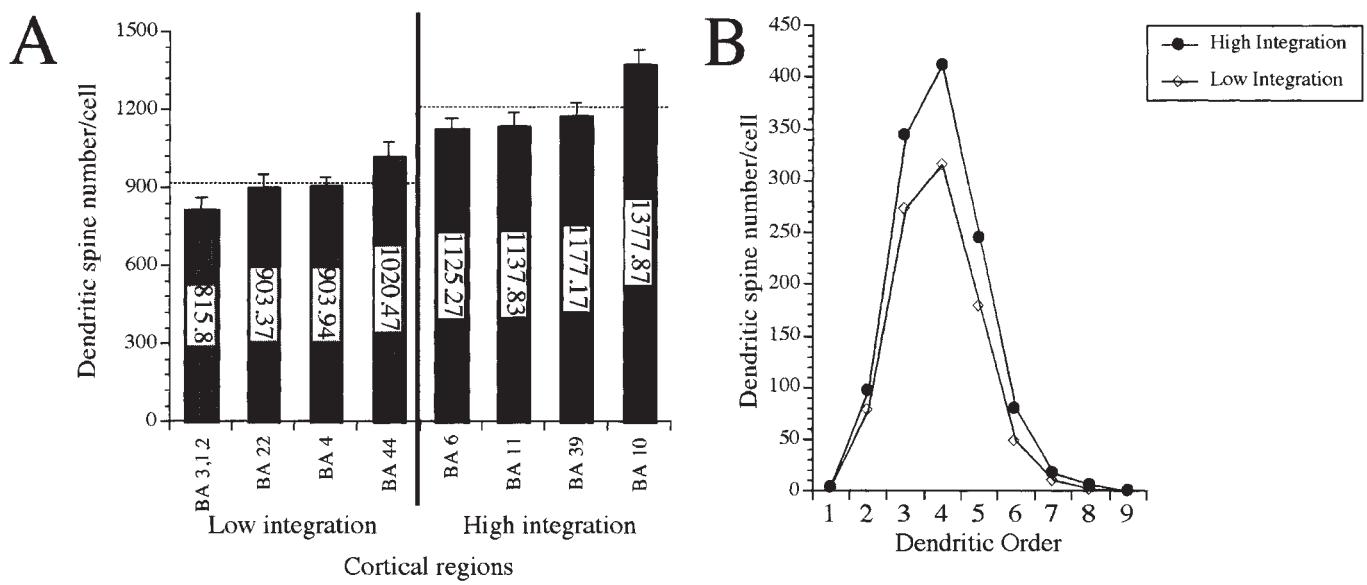

Figure 8. (*A*) Bar graph of the dendritic spine number (DSN) for each Brodmann area (BA), arranged from lowest (BA3-1-2) to highest (BA10). Areas have been characterized as low (BA3-1-2, BA22, BA4 and BA44) and high integration regions (BA6, BA11, BA39 and BA10), with the average DSN value for each grouping indicated by the dotted lines. Note the considerably higher DSN values for the high integration regions over the low integration regions. Error bars represent SEM. (*B*) Dendritic envelopes for low and high integration regions indicating the greatest differences in third-, fourth- and fifth-order dendritic branches.

for this underestimation, such techniques were not feasible here because spines were quantified along the entire basilar dendritic array rather than along short (i.e. 50 μm) segments of uniform diameter. Importantly, the present underestimation of spines is likely to be greatest in those regions exhibiting more complex (and perhaps thicker) dendritic systems. Thus, the observed regional differences in both dendritic and spine measures may actually be greater than reported.

Individual Morphological/Cytoarchitectonic Variability

The eight regions examined in the current analysis were chosen not only to represent different levels in Benson's (Benson, 1993, 1994) hierarchy, but also because they could be identified consistently on the basis of anatomical landmarks. Nevertheless, extensive interindividual variability characterizes (human) brain tissue (Bartley *et al.*, 1997). This variation is particularly confounding when attempting to establish structure–function relationships because classical cytoarchitectonic maps (i) can be misinterpreted (Zeki, 1979); (ii) do not necessarily map isomorphically with gyral–sulcal morphology (Loftus *et al.*, 1995); (iii) are typically based on qualitative rather than quantitative criteria; and (iv) are limited to observations of only

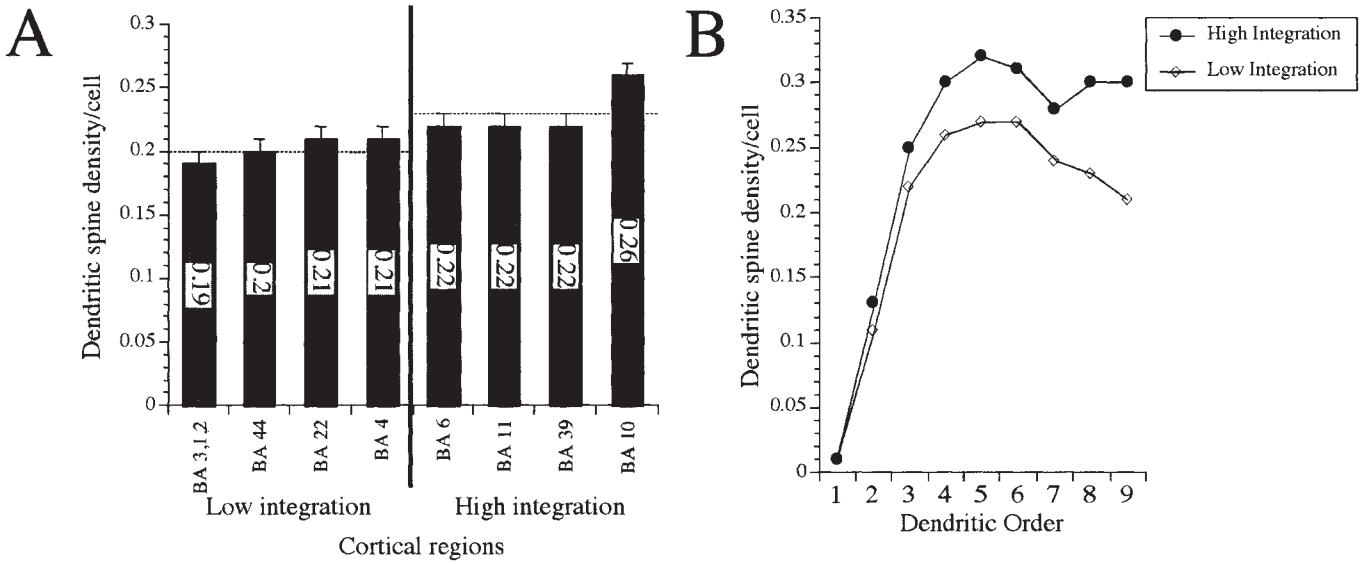

Figure 9. (*A*) Bar graph of the dendritic spine density (DSD) for each Brodmann area (BA), arranged from lowest (BA3-1-2) to highest (BA10). Areas have been characterized as low (BA3-1-2, BA44, BA22 and BA4) and high integration regions (BA6, BA11, BA39 and BA10), with the average DSD value for each grouping indicated by the dotted lines. Note the relatively higher DSD values for the high integration regions over the low integration regions. Error bars represent SEM. (*B*) Dendritic envelopes for low and high integration regions indicating somatofugal increases in DSD, with the greatest differences exhibited in more distal segments.

a few or even a single brain (Rajkowska and Goldman-Rakic, 1995a,b). Although modern quantitative, histochemical techniques have recently permitted objective mapping of cortical areas [e.g. BA9 and BA46 (Rajkowska and Goldman-Rakic, 1995a); BA44 and BA45 (Amunts *et al.*, 1999)], a definitive map of the human cortex has not been established. Laminar examination of Nissl stains from the sampled regions of the present study indicated these areas were, in general, cytoarchitectonically consistent with their designation. Nevertheless, without quantitative cytoarchitectonic verification of every region from every brain, the areas examined in the present investigation should be seen as close approximations to their designated Brodmann classification.

Hierarchical Classification of Cortical Tissue

The present study adopted Benson's (Benson, 1993, 1994) hierarchical schema, which was derived from clinical and anatomical correlations. This schema is generally consistent with earlier, anatomy-based hierarchies (e.g. Pandya and Kuypers, 1969; Jones and Powell, 1970) outlining a stepwise cortico-cortical progression along sensory-fugal gradients (Mesulam, 1998). However, such a serial perspective of cortical organization remains an acknowledged oversimplification because extensive parallel cortico-cortical and subcortico-cortical connections are crucial to information processing (Selemon and Goldman-Rakic, 1988). The complexity of such interconnections has been demonstrated most clearly in the visual system, where the original hierarchical configuration (Hubel and Wiesel, 1962) has been substantially modified with the addition of recursively interactive parallel networks (Felleman and Van Essen, 1991). Ultimately, these distributed systems are critical for a comprehensive mapping of all hierarchical configurations, including Benson's proposed schema (Bressler, 1995).

Accepting that complete incorporation of subcortical, limbic and parallel networks into the cortical hierarchy is beyond the scope of the present analysis, the primary and supramodal regions of the present schema are typically more clearly categorized than are the intervening regions. In the present study, for example, BA22 and BA44 could have been categorized as heteromodal rather than as unimodal regions—indeed, Benson (Benson, 1994) himself indicates their potentially polymodal nature. Unfortunately, such a determination cannot be made with certainty without detailed functional mapping of each cortical region. Thus, the current hierarchical schema should be viewed as a simplified heuristic for cortical processing; as such, progression along a proposed hierarchy may not be paralleled exactly by concomitant increases in dendritic field area.

Age and Gender Issues

The present sample included individuals of both genders over a relatively broad age range. Although there is little reason to expect significant gender-related differences in dendritic extent (Jacobs and Scheibel, 1993), significant age-related changes in dendritic/spine systems – similar to those in the present study – have been extensively documented (Jacobs *et al.*, 1997). In examining the dendritic/spine values of each brain in the present study, we noted no appreciable gender or age-related differences in regional patterns, suggesting that the obtained regional patterns are quite robust and may be present by early adolescence. Indeed, developmental positron emission tomography research indicates that the adult pattern (not adult values) of local cerebral metabolic rates for glucose, which appear closely associated with dendritic extent (Jacobs *et al.*, 1995), are typically obtained around the first year of life (Chugani *et al.*, 1987). We are currently examining regional dendritic/spine variation in infant tissue to determine when the adult pattern emerges.

Regional Differences in Dendritic/Spine Systems

The present results are generally consistent with the findings of Elston and Rosa, who documented progressive increases in basal dendritic complexity along hierarchically arranged visual pathways in the monkey (Elston *et al.*, 1996; Elston and Rosa, 1997, 1998a,b). Specifically, their findings suggest a stepwise

progression in dendritic/spine complexity, with the more rostrally located, spine-dense neurons integrating a wider range of modulatory input than the more caudally located, sparsely spined dendritic trees. Moreover, the present findings elaborate considerably on those of Jacobs *et al.* (Jacobs *et al.*, 1997), who documented in humans significantly more complex dendritic/spine systems in BA10 over BA18, again suggesting that the dendritic/spine systems of cortical areas involved in the initial stages of information processing are not as complex as those involved later in the processing stream. Below, we provide a brief overview of each region examined in the present analysis. The overview is far from exhaustive, but provides a general indication of the relationship between dendritic/spine extent and the general integrative nature of each area.

Low Integration Regions

As the initial cortical area for discriminating incoming somatosensory information, BA3-1-2 receives most of its input from the ventral posterior nuclei of the thalamus (Clark and Boggon, 1935), with additional, limited input from adjacent sensorimotor cortices (Jones and Powell, 1970). In an investigation of intrinsic axon collaterals within this region, Porter (1997) has noted that proximal basilar dendrites in BA2 pyramidal cells appear to be the primary target of the projections from BA3a. Insofar as proximal dendritic systems mature before more distal systems, these proximal connections are probably crucial to the relatively early functional maturation of this cortical region (Chugani *et al.*, 1987). As such, it is not surprising that BA3-1-2 in the present study generally exhibited the least complex dendritic/spine system of all regions examined. Consistent with the hierarchical predictions, the measures for BA3-1-2 (e.g. TDL = 3191 μm/cell; DSN = 816 spines/cell) were also less than those observed in BA18 (e.g. TDL = 3563 μm/cell; DSN = 933 spines/cell) of a comparable human population, namely the younger group (M_{age} = 34 years) of Jacobs *et al.* (Jacobs *et al.*, 1997).

In contrast to BA3-1-2, BA4 appears to be more richly interconnected, receiving projections from the ventrolateral thalamus (Wiesendanger and Wiesendanger, 1985) and synthesizing information from several cortical areas, including somatosensory, premotor, supplementary motor, parietal association and prefrontal cortices (Jones *et al.*, 1978). A more complex dendritic array in BA4 neurons would facilitate the synthesis of various sources of input, including processed proprioceptive and tactile information from layer II and III pyramidal neurons in BA3-1-2 (Porter, 1997), prior to initiating smooth voluntary movements. Indeed, BA4 neurons exhibited dendritic/spine systems of comparable or greater complexity than those of BA18 in Jacobs *et al.* (Jacobs *et al.*, 1997), or BA22 in the present study. Thus, BA4 neurons appear to be slightly more complex than predicted by Benson's functional hierarchy, suggesting that one should not group primary sensory and motor cortices together when comparing them at the morphological level.

In terms of unimodal regions, neurons in BA22 were slightly less complex than expected, ranking above only primary somatosensory cortex in complexity for most of the dendritic/spine measurements. The present dendritic measures for BA22 (e.g. TDL = 3302 μm/cell; DSN = 903 spines/cell) are greater than in previous reports for this region [TDL = 2672 μm/cell (Jacobs *et al.*,1993a); TDL = 2589 μm/cell (Jacobs *et al.*, 1993b); and TDL = 2239 μm/cell and DSN = 526 spines/cell (Anderson and Rutledge, 1996)], presumably because of differing subjects and quantification techniques. Dendritic/spine values for BA22 were nevertheless similar to those obtained by Jacobs *et al.* (Jacobs *et al.*, 1997) for another unimodal region, namely BA18 (TDL = 3563 μm/cell; DSN = 933 spines/cell). One possible explanation for the relatively low complexity of this region is that the present sampling criteria for BA22 placed it adjacent to primary auditory cortex, thus probably limiting it more to unimodal, auditory processing. Conceivably, a section more posterior along the superior temporal gyrus would be involved in synthesizing a greater proportion of polymodal information, especially given that the sensory speech region receives a wide sampling of cortical and subcortical input (Jones and Powell, 1970; Seldon 1985). In turn, a more posterior region might also have exhibited more complex dendritic ensembles.

Significantly connected with BA22 by the superior longitudinal and arcuate fasciculi (Krieg, 1963; Petrides and Pandya, 1988) is classical Broca's area, which was the most dendritically complex of all low integration regions. In fact, BA44 was the only low integration region to surpass a high integration region on one of the dendritic measures (recall Fig. 6*A*). Classification of this region as unimodal is itself problematic, however. Indeed, Benson (1994) classified BA44 as unimodal and the more anterior BA45 as heteromodal. Given the variability of these regions (Amunts *et al.*, 1999), it is possible that the sampled area in the present study was multimodally responsive, receiving not only auditory, but also visual, somesthetic and limbic input (Geschwind, 1965). The relatively complex dendritic ensembles in this region would thus assist in integrating the polymodal information required for generating the motor sequences involved in language output.

High Integration Regions

According to Mesulam (Mesulam, 1998), heteromodal regions represent 'epicenters' for large networks, with each epicenter potentially interacting with several other networks. The two heteromodal regions examined in the present study, BA6β and BA39, certainly fit this description and exhibited very similar levels of dendritic/spine complexity. The supplementary motor area constitutes a convergence zone for projections from primary and secondary sensorimotor cortices, parietal association cortex, the anterior cingulate gyrus and indirectly from the basal ganglia (Damasio *et al.*, 1981; Schell and Strick, 1984). This pattern of input suggests that BA6β integrates multimodal sensory information [except that of a visual nature (Pandya and Kuypers, 1969)] and limbic-mediated input in order to prepare, inhibit and/or modify (learned) motor programs for internally driven behavior (Orgogozo and Larsen, 1979). Synthesizing such a constellation of diverse input presumably requires the relatively complex dendritic/spine systems exhibited by this region.

Similarly, BA39 has been found to contain primarily multimodally responsive neurons involved in integrating information from several surrounding transitional fields and from subcortical regions (Hyvärinen and Shelepin, 1979; Eidelberg and Galaburda, 1984). At the cortical level, BA39 receives ipsilateral association fibers from frontal (motor, premotor and prefrontal), parietal, temporal and occipital lobes, and from the contralateral inferior parietal lobule (Hyvärinen, 1982a,b). Subcortical afferents originate in the thalamus (anterior and posterior nuclei and pulvinar), hippocampus, basal forebrain nuclei, claustrum, substantia nigra, locus coerueus and Raphé nuclei (Hyvärinen, 1982a,b). Neurons in this region are thus involved not only in polymodal integration, but in more abstract cognitive and symbolic functions such as spatial referencing, mental arithmetic and semantic memory (Démonet *et al.*, 1992; Roland,

1993). The true integrative nature of this region is revealed through lesions, which result in complex constellations of deficits such as Balint's and Gerstmann's syndromes.

In contrast to the two heteromodal regions, the two supramodal areas differed considerably from each other in terms of dendritic/spine complexity. For all measures (especially DSN and DSD), BA11 neurons were substantially less complex than BA10. Indeed, BA11 was the least complex of all high integration regions. BA10, however, exhibited the highest dendritic/spine values of all regions examined, values that were very similar to those reported by Jacobs *et al.* (Jacobs *et al.*, 1997). The reason for this discrepancy between BA10 and BA11 is unclear, although one could speculate that it reflects underlying differences in the type and/or degree of connectivity. Whereas the dorsolateral portion of the prefrontal cortex (including BA10) receives dense projections from the dorsal parietal cortex, the ventrolateral portion (including BA11) receives dense projections from inferotemporal cortex (Wilson *et al.*, 1993; Barbas, 1995). Moreover, given that the present sampling of BA11 borders the orbitomedial division of the prefrontal lobe, it is likely that it shares more direct anatomical connections with the amygdala and periamygdaloid cortical regions than BA10 (Cavada *et al.*, 2000; Öngür and Price, 2000), and thus may contribute particularly to the emotional evaluation of sensory experiences (Morecraft *et al.*, 1992; Barbas, 1995).

Regardless of potential differences in the interconnectivity patterns of BA10 and BA11, the dorsolateral prefrontal cortex remains one of the most richly integrative regions of the primate brain, receiving not only input from subcortical structures such as the dorsomedial thalamus (Goldman-Rakic and Porrino, 1985; Barbas *et al.*, 1991), but also higher order sensory information from parietal, temporal and occipital association areas (Jacobson and Trojanowski, 1977; Preuss and Goldman-Rakic, 1991). In particular, the majority of prefrontal supragranular pyramidal cells appear to receive substantial excitatory input from other prefrontal pyramidal neurons through long-distance axon collaterals (Melchitzky *et al.*, 1998). Moreover, these intrinsic connections appear to be greater than in posterior cortical regions (McGuire *et al.*, 1991; Lund *et al.*, 1993). Although frontopolar regions such as BA10 do not exhibit consistent co-activation patterns with specific behaviors or sensory input, these regions are crucially involved in higher-order orchestrations of cortical networks (Roland, 1984). Thus, dorsolateral prefrontal neurons, which display the selective, delayed firing crucial to maintaining internal representations of behaviorally relevant cues (Fuster 1973; González-Burgos *et al.*, 2000), are in a unique position to orchestrate top-down (i.e. sensory-petal) control of memory and attention mechanisms relevant to multiple perceptual and cognitive domains (Cabeza and Nyberg, 1997; Mesulam, 1998).

Complex dendritic/spine systems, particularly as expressed by BA10 pyramidal neurons, provide the necessary surface area for transmodal integration of such a broad spectrum of information. Indeed, the high spine values for BA10 in the present study are consistent with recent research in monkeys, which indicates that the basilar dendrites of prefrontal neurons are significantly more spiny than those in occipital, temporal or parietal cortices (Elston, 2000). Metabolic evidence provides additional support for the existence of complex dendritic arbors in the dorsolateral prefrontal region. Given that up to 80% of glucose utilization is devoted to maintenance of the Na^+/K^+ ion exchange across cell membranes (Sokoloff, 1977), and that dendrites may constitute >90% of a neuron's receptive surface area (Schadé and Baxter, 1960), it is not surprising that the dorsolateral prefrontal cortex (including BA10) typically exhibits higher metabolism and regional cerebral blood flow in the normal, resting state than do other cortical areas (Roland, 1984).

Dendritic Integration and Functional Implications

As indicated in the present study, the increase in total dendrite length in humans from primary cortical regions to supramodal areas is approximately one-third, and that of total spine number is about two-thirds. Both structural and physiological research suggests that such quantitative morphological differences may contribute to the robust qualitative differences assumed to exist between processing mechanisms in different cortical regions. Structurally, pyramidal cells communicate predominantly with each other through vertically recurrent collaterals and horizontal long-distance intrinsic projections (Winfield *et al.*, 1981; Douglas *et al.*, 1995). The primary targets of these intracortically derived connections appear to be the basilar dendrites (Globus and Scheibel, 1967a,b,c). Thus, progressive increases in basilar dendritic extent, as documented in the present study for high integration regions, might reflect the neurons' increased exposure to intracortical influences and participation in cortical networks, a relationship that intuitively meets assumptions about information convergence and increasingly more complex associative functions.

Physiologically, dendritic systems appear to be highly compartmentalized, independent subunits, whose morphological and membrane characteristics crucially determine a cell's input–output transformations (Helmchen, 1999; Spruston *et al.*, 1999). These dendrites dynamically sample surrounding areas for correlated activity (Katz *et al.*, 1989; Kossel *et al.*, 1995), and integrate it with a complex repertoire of nonlinear, active, electrochemical responses that provide considerable computational flexibility (Quartz and Sejnowski, 1997). These active characteristics boost the effect of (distal) synaptic input, contributing significantly to synaptic integration locally and across the entire neuron. Consequently, the fine, outermost branches of the dendrite ensemble – such as those in high integration regions – may assume physiological importance out of proportion to the modest fraction of the dendritic ensemble they represent (Magee and Cook, 2000). Moreover, dendritic spines, which are generally more dense on distal than proximal segments (recall Fig. 9*B*), are crucial to this integration process insofar as the most peripheral spines are thought to be particularly effective in adjusting synaptic potency (Shepherd *et al.*, 1985). Thus, the excitability of an entire dendrite may be disproportionately regulated by changes in distal spine density (Jaslove, 1992). In summary, both anatomical and physiological evidence suggests that the dendritic/spine variations observed across diverse cortical regions in the present study contribute to the formation of integrative neural networks underlying complex cognitive processes (Knudsen, 1994; Yuste and Tank, 1996).

Conclusion

Quantitative neuromorphological investigations such as the present study substantially enhance our understanding of the dendritic ensembles first described in qualitative observations and set the stage for the development of a quantitative dendritic map of the cerebral cortex. Despite considerable inter-individual variation and inherent design limitations, clear regional differences in the predicted direction were revealed by the present quantitative analysis. Dendritic/spine systems in primary

(BA3-1-2 and BA4) and unimodal (BA22 and BA44) regions were consistently less complex than in heteromodal (BA6β and BA39) and supramodal (BA10 and BA11) areas. Dendritic/spine systems were thus significantly more complex in high integration regions than in low integration regions. Highest dendritic/spine values were in BA10, which exhibited 31% greater total dendritic length and 69% greater dendritic spine number than the least complex region, namely BA3-1-2. It seems likely that these regional variations reflect significant differences in the nature of cortical processing. Many other factors are undoubtedly involved in determining the range of computational strategems as one moves from first-level sensory representations to the highest associational levels. Nonetheless, the quantitative characteristics of the receptive dendritic membrane of individual neuronal elements and their variations along the length of the dendritic shaft appear to represent central issues in cortical computation and behavioral flexibility.

Notes

Partial support for this work was provided by the National Science Foundation's Division of Undergraduate Education grant (DUE-#9550790), the Hughes Foundation, the John D. and Catherine T. MacArthur Professorship, and The Colorado College's divisional research funds. Preliminary reports of some of these results have appeared in abstract form (Baca *et al.*, 1995; Prather *et al.*, 1997). We gratefully acknowledge David Bowerman, Al Correl, Richard Sherwin, Leroy Fischer, Edmund Orsini and Wes Tyson for their generous assistance with this project. We also thank several students who participated in data collection: Sherry Bekhit, Becca Kernan, Birgit Fisher, Jennifer Ferguson, Jon Driscoll and Kelly Courns. Finally, we dedicate this work with admiration to Dr. Arnold B. Scheibel.

Address correspondence to Bob Jacobs, Laboratory of Quantitative Neuromorphology, Department of Psychology, The Colorado College, 14 E. Cache La Poudre, Colorado Springs, CO 80903, USA. Email: bjacobs@coloradocollege.edu

References

Amir Y, Harel M, Malach R (1993) Cortical hierarchy reflected in the organization of intrinsic connections in macaque monkey visual cortex. J Comp Neurol 334:19–64.

Amunts K, Schleicher A, Bürgel U, Mohlberg H, Uylings HB, Zilles K (1999) Broca's region revisited: cytoarchitecture and intersubject variability. J Comp Neurol 412:319–341.

Anderson B, Rutledge V (1996) Age and hemisphere effects on dendritic structure. Brain 119:1983–1990.

Baca S, Larsen L, Fisher B, Kernan R, Schall M, Jacobs B (1995) Dendritic and spine analyses across hierarchically arranged areas of human neocortex: a quantitative Golgi study. Soc Neurosci 182.9 [Abstract].

Barbas H, Henion THH, Dermon CR (1991) Diverse thalamic projections to the prefrontal cortex in the rhesus monkey. J Comp Neurol 313:65–94.

Barbas H (1995) Anatomic basis of cognitive–emotional interactions in the primate prefrontal cortex. Neurosci Biobehav Rev 19:499–510.

Bartley AJ, Jones DW, Weinberger D (1997) Genetic variability of human brain size and cortical gyral patterns. Brain 120:257–269.

Belichenko PV, Dahlström A (1995) Studies of the 3-dimensional architecture of dendritic spines and varicosities in human cortex by confocal laser scanning microscopy and Lucifer Yellow micro-injections. J Neurosci Methods 57:55–61.

Benson DF (1993) Prefrontal abilities. Behav Neurol 6:75–81.

Benson DF (1994) The neurology of thinking. New York: Oxford Press.

Bok ST (1959) Histonomy of the cerebral cortex. Amsterdam: Elsevier.

Braak H (1980) Architectonics of the human telencephalic cortex. Berlin: Springer.

Bressler SL (1995) Large-scale cortical networks and cognition. Brain Res Rev 20:288–304.

Brodmann K (1909) Vergleichende Lokalisationlehre der Grosshirnrinde in ihren Prinzipien dargestellt auf Grund des Zellenbaues. Leipzig: J.A. Barth.

Cabeza R, Nyberg L (1997) Imaging cognition: an empirical review of PET studies with normal subjects. J Cogn Neurosci 9:1–26.

Cavada C, Compañy T, Tejedor J, Cruz-Rizzolo RJ, Reinoso-Suárez F (2000) The anatomical connections of the Macaque monkey orbitofrontal cortex. A review. Cereb Cortex 10:220–242.

Chugani HT, Phelps ME, Mazziotta JC (1987) Positron emission tomography study of human brain functional development. Ann Neurol 22:487–497.

Clark WEL, Boggon RH (1935) The thalamic connections of the parietal and frontal lobes of the brain in the monkey. Phil Trans R Soc Lond (Biol) 224:313–359.

Damasio AR, Van Hoesen GW, Vilensky J (1981) Limbic-motor pathways in the primate: a means for emotion to influence motor behavior. Neurology 31:60.

de Ruiter JP (1983) The influence of post-mortem fixation delay on the reliability of the Golgi silver impregnation. Brain Res 266:143–147.

Démonet J-F, Chollet F, Ramsay S, Cardebat D, Nespoulous JL, Wise R, Rascol A, Frackowiak R (1992) The anatomy of phonological and semantic processing in normal subjects. Brain 115:1753–1768.

Diamond MC, Krech D, Rosenzweig MR (1964) The effects of an enriched environment on the histology of the rat cerebral cortex. J Comp Neurol 123:111–119.

Douglas RJ, Kock C, Mahowald M, Martin KAC, Suarez HH (1995) Recurrent excitation in neocortical circuits. Science 269:981–985.

Eidelberg D, Galaburda AM (1984) Inferior parietal lobule: divergent architectonic asymmetries in the human brain. Arch Neurol 41: 843–852.

Elston GN (2000) Pyramidal cells of the frontal lobe: all the more spinous to think with. J Neurosci 20:1–4.

Elston GN, Rosa MGP (1997) The occipitoparietal pathway of the macaque monkey: comparison of pyramidal cell morphology in layer III of functionally related cortical visual areas. Cereb Cortex 7:432–452.

Elston GN, Rosa MGP (1998a) Complex dendritic fields of pyramidal cells in the frontal eye field of the macaque monkey: comparison with parietal areas 7a and LIP. NeuroReport 9:127–131.

Elston GN, Rosa MGP (1998b) Morphological variation of layer III pyramidal neurones in the occipitotemporal pathway of the macaque monkey visual cortex. Cereb Cortex 8:278–294.

Elston GN, Rosa MGP, Calford Mbyte (1996) Comparison of dendritic fields of layer III pyramidal neurons in striate and extrastriate visual areas of the marmoset: a Lucifer Yellow intracellular injection study. Cereb Cortex 6:807–813.

Feldman ML, Peters A (1979) Technique for estimating total spine numbers on Golgi-impregnated dendrites. J Comp Neurol 118: 527–542.

Felleman DJ, Van Essen DC (1991) Distributed hierarchical processing in the primate cerebral cortex. Cereb Cortex 1:1–47.

Flood DG (1993) Critical issues in the analysis of dendritic extent in aging humans, primates, and rodents. Neurobiol Aging 14:649–654.

Fuster JM (1973) Unit activity in prefrontal cortex during delayed-response performance: neuronal correlates of transient memory. J Neurophysiol 36:61–78.

Geschwind N (1965) Disconnection syndromes in animals and man. Brain 88:585–644.

Globus A, Scheibel AB (1967a) Pattern and field in cortical structure: The rabbit. J Comp Neurol 131:155–172.

Globus A, Scheibel AB (1967b) Synaptic loci on visual cortical neurons of the rabbit: the specific afferent radiation. Exp Neurol 18:116–131.

Globus A, Scheibel AB (1967c) Synaptic loci on parietal cortical neurons: termination of corpus callosum fibers. Science 156:1127–1129.

Goldman-Rakic PS, Porrino LJ (1985) The primate mediodorsal (MD) nucleus and its projections to the frontal lobe. J Comp Neurol 242:535–560.

González-Burgos G, Barrionuevo G, Lewis DA (2000) Horizontal synaptic connections in monkey prefrontal cortex: an *in vitro* electrophysiological study. Cereb Cortex 10:1047–3211.

Gridley M (1960) Manual of histologic and special staining techniques, 2nd edn. New York: McGraw-Hill.

Helmchen F (1999) Dendrites as biochemical compartments. In: Dendrites (Stuart G, Spruston N, Häusser M, eds), pp. 161–192. New York: Oxford University Press.

Hof PR, Mufson EJ, Morrison JH (1995) Human orbitofrontal cortex: cytoarchitecture and quantitative immunohistochemical parcellation. J Comp Neurol 359:48–68.

Horner CH, Arbuthnott E (1991) Methods of estimation of spine density — are spines evenly distributed throughout the dendritic field? J Anat 177:179–184.
Hubel DH, Wiesel TN (1962) Receptive fields, binocular interaction and functional architecture in the cat's visual cortex. J Physiol (Lond) 160:106–154.
Hyvärinen J (1982a) Posterior parietal lobe of the primate brain. Physiol Rev 62:1060–1129.
Hyvärinen J (1982b) The parietal cortex of monkey and man. Berlin: Springer.
Hyvärinen J, Shelepin Y (1979) Distribution of visual and somatic functions in the parietal association area of the monkey. Brain Res 169:561–564.
Jacobs B, Batal HA, Lynch B, Ojemann G, Ojemann L, Scheibel AB (1993a) Quantitative dendritic and spine analyses of speech cortices: a case study. Brain Lang 44:239–253.
Jacobs B, Schall M, Scheibel AB (1993b) A quantitative dendritic analysis of Wernicke's area in humans. II. Gender, hemispheric, and environmental factors. J Comp Neurol 327:97–111.
Jacobs B, Chugani HT, Allada V, Chen S, Phelps ME, Pollack DB, Raleigh MJ (1995) Developmental changes in brain metabolism in sedated rhesus macaques and vervet monkeys revealed by positron emission tomography. Cereb Cortex 5:222–233.
Jacobs B, Driscoll L, Schall M (1997) Life-span dendritic and spine changes in areas 10 and 18 of human cortex: a quantitative Golgi Study. J Comp Neurol 386:661–680.
Jacobs B, Scheibel AB (1993) A quantitative dendritic analysis of Wernicke's area in humans. I. Lifespan changes. J Comp Neurol 327:83–96.
Jacobson S, Trojanowski JQ (1977) Prefrontal granular cortex of the rhesus monkey. I. Intrahemispheric cortical afferents. Brain Res 132:209–233.
Jaslove SW (1992) The integrative properties of spiny distal dendrites. Neuroscience 47:495–519.
Jones EG, Powell TPS (1970) An anatomical study of converging sensory pathways with the cerebral cortex of the monkey. Brain 93:793–820.
Jones EG, Coulter JD, Hendry SHC (1978) Intracortical connectivity of architectonic fields in the somatic sensory, motor, and parietal cortex of monkeys. J Comp Neurol 181:291–348.
Katz LC, Gilbert CD, Wiesel TN (1989) Local circuits and ocular dominance columns in monkey striate cortex. J Neurosci 9: 1389–1399.
Knudsen EI (1994) Supervised learning in the brain. J Neurosci 14: 3985–3997.
Kossel A, Lowel S, Bolz J (1995) Relationships between dendritic fields and functional architecture in striate cortex of normal and visually deprived cats. J Neurosci 15:3913–3926.
Krieg WJW (1963) Connections of the cerebral cortex. Evanston: Brain Books.
Loftus WC, Tramo MJ, Gazzaniga MS (1995) Cortical surface modeling reveals gross morphometric correlates of individual differences. Hum Brain Mapp 3:257–270.
Lund JS, Yoshioka T, Levitt JB (1993) Comparison of intrinsic connectivity in different areas of macaque monkey cerebral cortex. Cereb Cortex 3:148–162.
Magee JC, Cook EP (2000) Somatic EPSP amplitude is independent of synapse location in hippocampal pyramidal neurons. Nature Neurosci 3:895–903.
McGuire BA, Gilbert CD, Rivlin PK, Wiesel TN (1991) Targets of horizontal connections in macaque primary visual cortex. J Comp Neurol 305:370–392.
Melchitzky DS, Sesack SR, Pucak ML, Lewis DA (1998) Synaptic targets of pyramidal neurons providing intrinsic horizontal connections in monkey prefrontal cortex. J Comp Neurol 390:211–224.
Mesulam M-M (1985) Principles of behavioral neurology. Philadelphia: F.A. Davis.
Mesulam M-M (1998) From sensation to cognition. Brain 121:1013–1052.
Morecraft RJ, Geula C, Mesulam M-M (1992) Cytoarchitecture and neural afferents of orbitofrontal cortex in the brain of the monkey. J Comp Neurol 323:341–358.
Öngür D, Price JL (2000) The organization of networks within the orbital and medial prefrontal cortex of rats, monkeys and humans. Cereb Cortex 10:206–219.
Orgogozo JM, Larsen B (1979) Activation of the supplementary motor area during voluntary movement in man suggests it works as a supramotor area. Science 206:847–850.
Pandya DN, Kuypers HG (1969) Cortico-cortical connections in the rhesus monkey. Brain Res 13:13–36.
Penfield W, Boldrey E (1937) Somatic motor and sensory representation in the cerebral cortex of man as studied by electrical stimulation. Brain 60:389–443.
Petrides M, Pandya DN (1988) Association fiber pathways to the frontal cortex from the superior temporal region in the rhesus monkey. J Comp Neurol 273:52–66.
Porter LL (1997) Morphological characterization of a cortico-cortical relay in the cat sensorimotor cortex. Cereb Cortex 7:100–109.
Prather M, Treml M, Driscoll L, Schall M, Jacobs B (1997) Regional variation in dendritic and spine complexity: a quantitative Golgi analysis of human cerebral cortex. Soc Neurosci 87.13 [Abstract].
Preuss TM, Goldman-Rakic PS (1991) Ipsilateral cortical connections of granular frontal cortex in the strepsirhine primate *Galago*, with comparative comments on anthropoid primates J Comp Neurol 305:507–549.
Quartz SR, Sejnowski TJ (1997) The neural basis of cognitive development: a constructivist manifesto. Behav Brain Sci 20: 537–596.
Rajkowska G, Goldman-Rakic PS (1995a) Cytoarchitectonic definition of prefrontal areas in the normal human cortex: I. Remapping of areas 9 and 46 using quantitative criteria. Cereb Cortex 5:307–322.
Rajkowska G, Goldman-Rakic PS (1995b) Cytoarchitectonic definition of prefrontal areas in the normal human cortex: II. Variability in locations of areas 9 and 46 and relationship to the Talairach coordinate system. Cereb Cortex 5:323–337.
Ramón y Cajal S (trans. by L. Azoulay) (1894) Les nouvelles ideés sur la structure du système nerveux chez l'homme et chez les vertébrés. Paris: Reinwald.
Ramón y Cajal S (trans. by L. Azoulay) (1909, 1911) Histologie du système nerveux de l'homme et des vertébrés, 2 vols. Paris: Maloine.
Ramón-Moliner E (1962) An attempt at classifying nerve cells on the basis of their dendritic patterns. J Comp Neurol 119:211–227.
Roland PE (1984) Metabolic measurements of the working frontal cortex in man. Trends Neurosci 7:430–435.
Roland PE (1993) Brain activation. New York: John Wiley & Sons.
Sanides F (1962) Die Architektonik des menschlichen Stirnhirns. Berlin: Springer Verlag.
Sastre-Janer FA, Regis J, Belin P, Mangin J-F, Dormont D, Masure M-C, Remy P, Frouin V, Samson Y (1998) Three-dimensional reconstruction of the human central sulcus reveals a morphological correlate of the hand area. Cereb Cortex 8:641–647.
Schadé JP, Baxter CF (1960) Changes during growth in the volume and surface area of cortical neurons in the rabbit. Exp Neurol 2:158–178.
Scheibel ME, Scheibel AB (1978) The methods of Golgi. In: Neuroanatomical research techniques (Robertson RT, ed.), pp. 89–114. New York: Academic Press.
Scheibel AB, Paul LA, Fried I, Forsythe AB, Tomiyasu U, Wechsler A, Kao A, Slotnick J (1985) Dendritic organization of the anterior speech area. Exp Neurol 87:109–117.
Scheibel AB, Conrad T, Perdue S, Tomiyasu U, Wechsler A (1990) A quantitative study of dendrite complexity in selected areas of the human cerebral cortex. Brain Cogn 12:85–101.
Schell GR, Strick PL (1984) The origin of thalamic inputs to the arcuate premotor and supplementary motor areas. J Neurosci 4:539–60.
Seldon HL (1985) The anatomy of speech perception: Human auditory cortex. In: Cerebral cortex (Peters A, Jones EG, eds), vol. 4, pp. 273–327. New York: Plenum Press.
Selemon LD, Goldman-Rakic PS (1988) Common cortical and subcortical targets of the dorsolateral prefrontal and posterior parietal cortices in the rhesus monkey: evidence for a distributed neural network subserving spatially guided behavior. J Neurosci 8:4049–4068.
Shepherd GM, Brayton RK, Miller JP, Segev I, Rinzel J, Rall W (1985) Signal enhancement in distal cortical dendrites by means of interactions between active dendritic spines. Proc Natl Acad Sci USA 82:2192–2195.
Sokoloff L (1977) Relation between physiological function and energy metabolism in the central nervous system. J Neurochem 29:13–26.
Spruston N, Stuart G, Häusser M (1999) Dendritic integration. In: Dendrites (Stuart G, Spruston N, Häusser M, eds), pp. 231–270. New York: Oxford University Press.
Uylings HBM, Ruiz-Marcos A, van Pelt J (1986) The metric analysis of

three-dimensional dendritic tree patterns: a methodological review. J Neurosci Methods 18:127–151.
Van Hoesen GW, Parvizi J, Chu C-C (2000) Orbitofrontal cortex pathology in Alzheimer's disease. Cereb Cortex 10:243–251.
Vogt O (1910) Die myeloarchitektonische Felderung des menschlichen Stirnhirns. J Psychol Neurol 15:221–232.
von Economo C, Koskinas GN (1925) Die Cytoarchitektonik der Hirnrinde des erwachsenen Menschen. Berlin: Springer.
Wiesendanger R, Wiesendanger M (1985) Cerebello-cortical linkage in the monkey as revealed by transcellular labeling with the lectin wheat germ agglutinin conjugated to the marker horseradish peroxidase. Exp Brain Res 59:105–117.
Williams RS, Ferrante RJ, Caviness VS Jr. (1978) The Golgi rapid method in clinical neuropathology: morphological consequences of suboptimal fixation. J Neuropathol Exp Neurol 37:13–33.
Wilson FA, Scalaidhe SP, Goldman-Rakic PS (1993) Dissociation of object and spatial processing domains in primate prefrontal cortex. Science 260:1955–1958.
Winfield DA, Brooke RNL, Sloper JJ, Powell TPS (1981) A combined Golgi-electron microscopic study of the synapses made by the proximal axon and recurrent collaterals of a pyramidal cell in the somatic sensory cortex of the monkey. Neuroscience 6: 1217–1230.
Yuste R, Tank DW (1996) Dendritic integration in mammalian neurons, a century after Cajal. Neuron 16:701–716.
Zeki SM (1979) Zu Brodmann Area 18 und 19. Exp Brain Res 36:195–197.